Photothermal deflection method for monitoring photoelectronic and nonradiative energy conversion in semiconductor photoelectrochemical cells

Robert E. Wagner and Andreas Mandelis
Photoacoustic and Photothermal Sciences Laboratory, Department of Mechanical Engineering, and Laser and Lightwave Research Center, University of Toronto, Toronto, Canada M5S 1A4
(Received 4 May 1988)

By employing an extended model for heat generation in a photoelectrochemical (PEC) cell, an expression for the photothermal deflection (PD) signal at the working electrode of a PEC cell is developed. Furthermore, several experimental PD-signal–versus–bias-voltage curves are presented for three low-resistivity CdS–polysulfide-electrolyte PEC cells. The experimental PD-signal–versus–bias data are then used to obtain the photocurrent quantum efficiencies of the PEC cells at reverse bias and electronic energy-level parameters of the photoelectrochemical interface, making use of a simple, theoretical relationship between the slope of the PD-bias curve and the quantum efficiency; the quantum efficiencies were found to lie within the range 0.05–0.45, reasonable values given that the crystals were found to form current-inhibiting corrosion layers at reverse bias. A general discussion regarding the usefulness of the PD technique in obtaining quantitative PEC energy-conversion parameters is also included, with special emphasis on photogenerated species gradient perturbations.

INTRODUCTION

Photothermal deflection spectroscopy (PDS) is a well-known thermal-wave technique[1,2] which is well suited to qualitatively measuring the optical-absorption spectra, *in situ,* of photoelectrochemical (PEC) electrodes.[3] PDS employs a probe laser beam, propagating parallel to the working electrode (WE) surface, to detect the temperature (refractive index) gradient which exists perpendicular to an electrode being excited with intensity modulated light. The light absorbed by the WE is normally converted to heat by the efficient nonradiative deexcitation of the nonequilibrium, optically generated, electron-hole pairs. Due to the presence of the temperature or refractive index gradient at the WE-electrolyte interface, the probe beam will undergo a deflection which can be measured with a position-sensitive photodetector; usually only the ac signal component is monitored, using lock-in detection, for signal-to-noise ratio (SNR) enhancement. If the relative spectral content of the exciting beam is maintained constant, the PDS signal is found to be a linear function of the maximum illumination intensity;[2] thus, the PDS technique can be employed as a microcalorimetric probe to measure the relative degree of heating at the WE-electrolyte interface. When the illuminated WE is dc biased, heat generation within the electrode becomes relatively more complex, but a model has been developed[4] which quantifies the electrode heating under this condition; in this work, this model has been modified for the situation where a probe laser beam is used to detect the degree of WE heating. Also, following the work of Fujishima *et al.*,[4] a method for determining the PEC photocurrent quantum efficiency from PDS signal–versus–bias-voltage plots has been developed. Finally, an expression for the PDS signal for a PEC cell operated under load has been established, and the possibility of determining the energy-conversion efficiency from these measurements will be discussed.

As a means of testing the PDS bias model, experiments were carried out on three different low-resistivity CdS electrodes in polysulfide electrolyte. CdS, a direct-gap II-VI compound semiconductor, has been the subject of many PEC studies;[5,6] both solid-state[7] and solid-electrolyte[5,6] junction devices have been built which efficiently convert high-energy photons (photon energy greater than the approximately 2.4 eV band gap) to electrical energy. Electronically, CdS is a relatively complex material, and can contain a wide range of electronically active native and impurity defects.[8,9] Thus, even chemically "pure" materials can exhibit a wide variation in optical and electronic properties. In a PEC environment the situation is further complicated by the fact that corrosion layers may form on the electrode surface, altering the behavior of the electrode-electrolyte junction; in all cases corrosion was found to occur to a certain extent, resulting in quantum efficiency values less than 0.5.

THEORY

For the development of a PEC cell photothermal laser beam deflection model, the following assumptions are made. (a) The working electrode absorbs N photons per unit time at peak excitation (and for a modulation frequency of f, $N/2f$ photons per cycle), each with an energy $h\nu$. Photons not absorbed by the electrode, due to transmission or reflection, are lost to the system and cannot be accounted for by PDS or photocurrent measurements. The model is only valid for situations where fundamental [valence band (VB) to conduction band (CB)] electronic transitions constitute the dominant optical-absorption process. (b) No corrosion takes place at the WE while measurements are being carried out, and the electrochemical reactions which occur at the WE are as-

sumed not to vary with time. (c) All heat-generating processes at the WE contribute to the PDS signal through the same proportionality constant, K, a complex function of geometry and several system parameters. The previous statement is equivalent to saying that all of the heating processes have the same temporal and spatial distributions; this assumption is generally valid for the WE, where most of the heating takes place very close to the electrode-electrolyte interface (within one thermal diffusion length[3] of the interface), and most of the deexcitation processes occur very soon after optical absorption. (d) None of the optically generated electron-hole pairs recombine radiatively. Therefore, if Q is the quantum efficiency for current generation, QN carriers contribute to the maximum photocurrent, and $(1-Q)N$ carriers recombine nonradiatively.

Now, our goal is the quantification of heat generating processes in the PEC cell under two different experimental conditions: (a) The cell is illuminated with chopped light while a dc bias is applied across the WE and counter electrode (CE), and (b) the WE and CE are connected across a load resistor under chopped light illumination. These two situations are fundamentally different for the following reason: The biased cell is effectively short circuited, and the photocurrent drops to zero during that part of the illumination cycle when the light is blocked; on the other hand, when the cell is operated under load, a significant photocurrent will exist even when the exciting light has been blocked, owing to the slow kinetics of the PEC cell under load conditions.[10]

Employing the formalism of Fujishima *et al.*[4] and Maeda *et al.*,[11] the significant thermal processes at the WE-electrolyte interface are represented in the schematic diagram of Fig. 1. Quantitative expressions for the partial contributions of each of these processes to the PDS signal are now developed. The following expressions are extensions of those of Maeda *et al.*,[11] who derived relations pertaining to the experimentally similar thermistor photothermal spectroscopy: For the PEC cell under dc bias, expressions similar to Maeda *et al.* have been obtained, whereas for the cell under load, an extended set of relationships was derived which took into account both the ac and dc components of the cell photocurrent. The heat sources are as follows. (i) Following optical absorption, nonradiative intraband deexcitation of hot electrons from higher states in the conduction band to states near the band edge yields a signal component[11]

$$\Delta_1 = KN(h\nu - E_g) , \tag{1}$$

where E_g is the optical band gap of the semiconductor WE, and K is a geometry-dependent proportionality constant. All optically generated CB electrons are assumed to undergo this fast transition. (ii) Nonradiative interband deexcitation between the CB and VB contributes a signal component, under bias, of magnitude[11]

$$\Delta_2 = KN(1-Q_B)E_g , \tag{2}$$

where $Q_B = I_B/N$, where N is the peak photon flux (photons/sec), and I_B is the peak cell photocurrent, during a cycle (the unit for current has been chosen to be electrons/sec, unless otherwise noted). Under load conditions, a slightly different expression is obtained:

$$\Delta_2 = KN(1-Q_L^{ac}-Q_L^{dc})E_g , \tag{3}$$

where Q_L^{ac} $(=I_L^{ac}/N)$ is the ac component of the cell quantum efficiency, and I_L^{ac} is the ac component of the cell photocurrent; also, Q_L^{dc} $(=I_L^{dc}/N)$ is the dc component of the cell quantum efficiency, and I_L^{dc} is the dc component of the cell photocurrent. (iii) Electron injection from electrolyte species into the VB (for n-type electrode) gives, under bias,[11]

$$\Delta_3 = KNQ_B(E_R - E_{VB}^S) , \tag{4}$$

where E_R is the redox level of the electrolyte (versus reference), and E_{VB}^S is the valence-band energy level at the surface (versus reference). Under load conditions we obtain

$$\Delta_3 = 2KNQ_L^{ac}(E_R - E_{VB}^S) . \tag{5}$$

Note that the factor of 2 in Eq. (5) follows from the ac nature of Q_L^{ac}. (iv) Carrier separation in the depletion layer, during which the carriers lose energy under the influence of the built-in field, yields, for the biased electrode,[11]

$$\Delta_4 = KNQ_B q(V - V_{FB}) , \tag{6a}$$

$$= KNQ_B(E_{CB}^S - E_{CB}) , \tag{6b}$$

where V is the applied bias (versus reference), V_{FB} is the flatband potential (versus reference), E_{CB}^S is the conduction-band energy level at the surface (versus reference), and E_{CB} is the conduction-band energy level in the neutral bulk (versus reference). In developing Eqs. (6) the Fermi level of the semiconductor has been assumed to lie very close to the conduction-band edge, a good approximation for an n-type material. Under load conditions the situation is more complex:

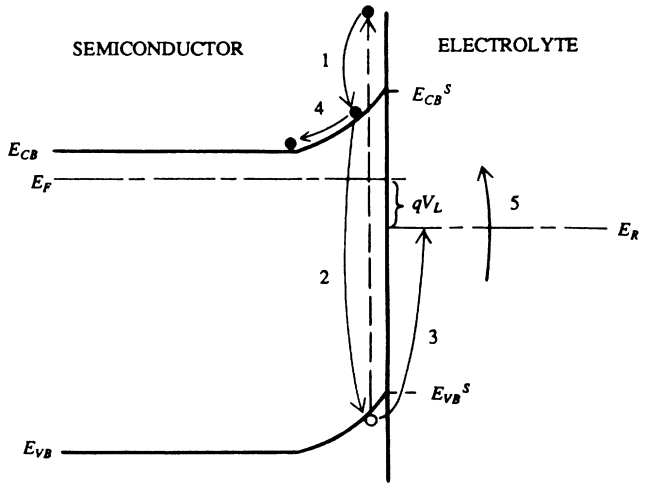

FIG. 1. Heat-generating mechanisms which contribute to the PDS signal at the working electrode-electrolyte interface (Ref. 11); refer to text for an explanation of the five heat sources (Δj; $j=1-5$).

$$\Delta_4 = KN[2Q_L^{ac}(E_{CB}^S - E_R - E_L^{dc}) - 2Q_L^{dc}E_L^{ac}] , \quad (7)$$

where $E_L^{dc} \equiv V_L^{dc}q$, and V_L^{dc} is the load voltage dc component. Furthermore, $E_L^{ac} \equiv V_L^{ac}q$, where V_L^{ac} is the load voltage ac component. (v) The free-energy change of the redox reaction, a significant part of the electrochemical Peltier heat (EPH) (Ref. 4), gives for the biased cell[11]

$$\Delta_5 = KNQ_B\Delta G , \quad (8)$$

where ΔG is the free-energy change of the WE redox reaction. For the cell under load we get

$$\Delta_5 = 2KNQ_L^{ac}\Delta G . \quad (9)$$

Finally, the resistive heating of the electrode and electrolyte can be ignored for a low-resistivity crystal and nondilute electrolyte.

When the five partial PDS signals for a cell under an applied bias are summed up, the total PDS signal can be written as

$$\Delta(V) = KN[(h\nu - E_g) + (1-Q)E_g + Q(E_R - E_{VB}^S) + Qq(V - V_{FB}) + Q\Delta G] , \quad (10)$$

where Q_B has been replaced by Q. If the cell is at open circuit, the quantum efficiency Q is zero. Thus, the PDS signal is

$$\Delta_{OC} = KNh\nu . \quad (11)$$

The open-circuit PDS signal provides a convenient means for normalizing the PDS signal under bias, since under open-circuit (OC) conditions all of the absorbed optical energy is converted to heat at the electrode-electrolyte interface. It should be noted that Q is an internal quantum efficiency; the concept of the internal quantum efficiency stems from the fact that the PDS signal under bias is normalized by the OC PDS signal. Since neither signal is sensitive to the absolute number of photons incident upon the WE, but only to the absorbed fraction, PDS measurements can only yield an internal quantum efficiency. Taking into account that K and N do not depend upon whether the system is at OC or under bias, Eqs. (10) and (11) yield an expression for the normalized PDS signal under bias:

$$\Delta(V)/\Delta_{OC} = [(h\nu - E_g) + (1-Q)E_g + Q(E_R - E_{VB}^S) + Qq(V - V_{FB}) + Q\Delta G]/h\nu . \quad (12)$$

Considering that the cell photocurrent and, hence, quantum efficiency are independent of bias at large reverse bias, we note that if we vary V within this region, Eq. (12) yields a slope of

$$\frac{\partial[\Delta(V)/\Delta_{OC}]}{\partial(V - V_{FB})} = \frac{qQ_{max}}{h\nu} , \quad (13)$$

where Q_{max} is defined as the maximum internal quantum efficiency of the PEC cell under given experimental conditions. The value of q, the electronic charge, on the right-hand side of Eq. (13), can be set to one if the unit of $h\nu$ is chosen to be eV. Equation (13) suggests a method for measuring the internal quantum efficiency of the PEC cell under monochromatic excitation from the slope of the normalized PDS-signal versus the applied bias.

Once Q_{max} has been found, it is possible to obtain an approximate value for the energy change in the system due to the redox reaction, namely, a value for $(E_R - E_{VB}^S) + \Delta G$, where $E_R - E_{VB}^S$ is the change in energy of an electron moving from the redox level to the VB, and ΔG is the free-energy change of the WE reaction. The quantity $(E_R - E_{VB}^S) + \Delta G$ is experimentally determined from the ordinate intercept of the $\Delta(V)/\Delta_{OC}$ versus $V - V_{FB}$ curve, which is given by

$$\Delta_{intercept} = [h\nu - Q_{max}E_g + Q_{max}(E_R - E_{VB}^S) + Q_{max}\Delta G]/h\nu . \quad (14)$$

Since the values of $h\nu$, E_g, and Q_{max} are nominally known, the value of $(E_R - E_{VB}^S) + \Delta G$ can be derived.

In order to find the quantum efficiency for current generation as a function of applied bias, a general expression for Q will first be written, noting that Q is defined as the number of electrons per unit time passing through the external PEC cell circuit (ignoring the dark current) divided by the number of photons absorbed by the electrode per unit time:

$$Q = (N_A/F)I/N , \quad (15)$$

where N_A is Avogadro's number, F is one faraday (1 faraday $= 10^4$ C/mole), I is the cell photocurrent in amperes, and N is the photon flux. Expressions for $Q(V)$, the quantum efficiency for the biased cell, and Q_{max}, the maximum cell quantum efficiency under high reverse bias, can be written using Eq. (15). Noting that N_A, F and N are independent of bias, $Q(V)$ can be written as a function of $I(V)$, I_{max}, and Q_{max}:

$$Q(V) = [I(V)/I_{max}]Q_{max} , \quad (16)$$

where I_{max} is the maximum photocurrent corresponding to Q_{max}. If Eq. (16) and the experimentally determined value of $(E_R - E_{VB}^S) + \Delta G$ are used in conjunction with the theoretical model for $\Delta(V)/\Delta_{OC}$ versus $V - V_{FB}$, Eq. (12), it becomes possible to compare the experimental and semitheoretical $\Delta(V)/\Delta_{OC}$ curves. The reason the term "semitheoretical" has been employed to describe the calculated $\Delta(V)/\Delta_{OC}$ curve is that the value of $(E_R - E_{VB}^S) + \Delta G$ substituted into Eq. (16) was obtained from experimental $\Delta(V)/\Delta_{OC}$ data, rather than from theory; therefore, the value of $(E_R - E_{VB}^S) + \Delta G$ was actually an adjustable parameter which guaranteed the coincidence of the experimental and semitheoretical PDS curves in the high-bias region.

A heat-generation model can also be formulated for the PEC cell connected to an external load resistor. Using the already derived partial heat generation terms for the cell under load, a relation for Δ_L/Δ_{OC} can be written

$$\Delta_L/\Delta_{OC} = [h\nu + (Q_L^{ac} - Q_L^{dc})E_g - 2(Q_L^{ac}E_L^{dc} + Q_L^{dc}E_L^{ac}) + 2Q_L^{ac}\Delta G]/h\nu , \quad (17)$$

where all quantities have been defined previously.

Cahen[12] has employed the experimentally related technique of photoacoustic spectroscopy (PAS) to find the internal energy-conversion efficiency of a solid-state photovoltaic cell, using a relation which links the PAS signal to the energy efficiency of a photovoltaic cell (ϵ_{PAS}):

$$\epsilon_{PAS}=(\Sigma_{OC}-\Sigma_L)/\Sigma_{OC} , \tag{18}$$

where Σ_{OC} is the PAS signal at open circuit and Σ_L is the PAS signal for the cell under load. Equation (18) follows from the expressions which can be derived for Σ_L and Σ_{OC}:

$$\Sigma_L=K'(h\nu-Q_L E_L) , \tag{19}$$

$$\Sigma_{OC}=K'h\nu , \tag{20}$$

where K' is a geometry-related factor, Q_L is the quantum efficiency of the cell under steady illumination, and $E_L \equiv qV_L$, where V_L is the load voltage under steady illumination. When Eqs. (19) and (20) are substituted into Eq. (18) the following expression is obtained:

$$\epsilon_{PAS}=Q_L E_L/h\nu \tag{21}$$

which can be obtained independently from the general definition of the electrical energy-conversion efficiency of a photovoltaic cell. The expression for Σ_L, for a solid-state photovoltaic cell, is much simpler than that for Δ_L, for a PEC cell: First, the solid-state system has no ΔG term, since no chemical reactions occur in the solid-state system; second, at lower modulation frequencies solid-state photovoltaic devices are normally quite "fast"—when the exciting light is momentarily blocked the photocurrent (PC) will drop to zero, and when the excitation is highest the PC will approach its steady-illumination value. Thus, for a solid-state cell it is not necessary to have separate ac and dc components for the load current and voltage. When expressions for Δ_L and Δ_{OC} are substituted into an equation like Eq. (18), we get

$$(\Delta_{OC}-\Delta_L)/\Delta_{OC}=[2(Q_L^{ac}E_L^{dc}+Q_L^{dc}E_L^{ac})-(Q_L^{ac}-Q_L^{dc})E_g -2Q_L^{ac}\Delta G]/h\nu . \tag{22}$$

If $Q_L^{ac}=Q_L^{dc}=0.5Q_L$, and $E_L^{ac}=E_L^{dc}=0.5E_L$, as is the case for solid-state photovoltaic cells, Eq. (22) reduces to

$$(Q_L E_L-Q_L\Delta G)/h\nu , \tag{23}$$

which is very close to Eq. (21), except for the presence of the ΔG term, as discussed above.

EXPERIMENT

For the sake of brevity, the three CdS samples will now be referred to by the following labels (1) pure low resistivity, LR-CdS, (2) F-doped, F-CdS, and (3) Ga-doped, Ga-CdS. All three crystals were obtained from Eagle-Picher, Inc. (Miami, OK). Since all samples were grown from high-temperature melts or vapors, they were assumed to have the wurtzite hexagonal structure. The LR-CdS sample was grown by the chemical vapor transport method described elsewhere.[9] The doped materials (F-CdS and Ga-CdS) were grown by crystal pulling from a melt in a carbon crucible, with the dopants present in the melt. All of the crystals were of *n* type, which is almost always the case for CdS.[8]

The LR-CdS sample measured $10\times10\times0.5$ mm^3 and had its optic axis parallel to its exposed face; its nominal resistivity was 4.75 Ω cm.[13] Originally the LR-CdS was 2 mm thick but it was polished down to one-quarter of its original thickness in an alumina-water slurry. The F-CdS crystal contained 0.01% F,[13] and measured $9\times6\times1.5$ mm^3; its exposed face was of unknown orientation. Fluorine atoms are known to form donors when incorporated into the CdS lattice.[14] The Ga-CdS sample contained 100 ppm Ga (Ref. 13) and measured $10\times10\times2$ mm^3; it was also of unknown orientation. Gallium atoms are also known to form donors in CdS.[14] Both of the doped samples were cut from cylindrical boules using a thin diamond-edged copper circular saw and polished in an alumina-water slurry. The pure sample was known to be a single crystal, but the doped samples were cut from boules of unknown quality and were not positively identified as single crystals.

Several steps were required to build operational working electrodes from the polished crystals. First, the crystals were etched in 3*M* HCl in order to remove as much of the surface damage layer as possible; the 20-sec etch was followed by a rinse in distilled water. Second, a bead of semiliquid indium-gallium amalgam was rubbed onto the back of each crystal, opposite the face which was to be exposed to the electrolyte. Smith[15] was shown that simple pressure contact results in a good ohmic junction between the In-Ga mixture and the CdS crystal. Third, each crystal was epoxied (DEVCON 5 *Minute*) onto an acrylic backing such that all surfaces of the crystal except the front face would be insulated. Finally, a copper wire was contacted to the In-Ga bead on each crystal back via a hole in the acrylic backing; this contact was then insulated by filling the access hole with epoxy. The working electrodes were periodically etched in HCl to remove corrosion products. The PEC cell counter-electrode, a piece of platinum foil covered in Pt black in order to increase its effective surface area, had a projected surface area of about 6 cm^2; the Pt electrode seemed to be inert in the corrosive polysulfide electrolyte. The potential of the WE was monitored with respect to a saturated calomel electrode (SCE).

With respect to our choice of cell electrolyte, we decided upon a polysulfide solution. Our electrolyte was expected to satisfy several requirements: Photoanodic corrosion of the electrode should be inhibited; this type of corrosion leads to the formation of a passivating sulfur layer on the crystal when anodic current is passed through the electrode under illumination:

$$CdS+h\nu\rightarrow Cd_{aq}^{2+}+S_s+2e^- . \tag{24}$$

The electrolyte should also be transparent to the light which is used to excite the electrode, and the electrolyte should provide a reversible redox reaction whereby the species oxidized at one electrode would be reduced at the other. According to Ellis *et al.*,[5,6] and Karas and Ellis,[16] polysulfide electrolyte (Na_2S, S, and NaOH in distilled water) was found to quench the anodic corrosion of CdS

up to a certain current density; also, under steady current flow the electrolyte composition remained fairly constant. Unfortunately, the large amount of sulfur (1.5M S to 1.0M Na_2S) recommended by Hodes[17] to stop corrosion would yield a solution opaque to the shorter visible wavelengths. Taking the above factors into account, we employed two similar polysulfide electrolytes: (i) 1.0M Na_2S, 0.01M S, and 1M NaOH in distilled water proved to be quite transparent, and (ii) 1.0M Na_2S, 0.05M S, and 1M NaOH in distilled water was more opaque than the former solution, but it provided better corrosion protection. The two solutions will henceforth be referred to as 0.01M PS and 0.05M PS, respectively. The solutions were prepared from: (i) sodium sulfide, 9-hydrate crystal (Na_2S-9H_2O), J. T. Baker, "Baker Analyzed"; (ii) sublimed sulfur powder, U.S.P., J. T. Baker, (iii) sodium hydroxide pellets (NaOH), 98.3%NaOH, J. T. Baker, "Baker Analyzed"; and (iv) distilled water. After the completion of our work we discovered a paper by Licht and Manassen[18] which claimed that NaOH does not serve any useful purpose in the polysulfide electrolyte, and can be excluded from the solution. Polysulfide electrolytes are known to decompose in air, and should be argon purged to remove dissolved oxygen; we did not purge our solutions but they were kept in airtight containers and discarded after a few days of use.

The three cell electrodes and the electrolyte were contained in an airtight acrylic cell. The cell featured three windows, one to allow the entry of the exciting optical beam, and two to allow the entry and exit of the PDS probe laser beam. Other important parts of the experimental apparatus are as follows. Optical excitation was carried out by means of an Oriel 8540 1000-W xenon lamp in an Oriel 6141 housing; the lamp was equipped with a photofeedback system to stabilize its power output. The lamp output was focused onto the input aperture of an Instruments S.A., Inc. monochromator, equipped with a diffraction grating blazed in the infrared. The 4-mm monochromator slits provided an optical bandwidth of about 16 nm. The lamp beam from the monochromator was periodically modulated with a PRA OC 4000 mechanical chopper. Three ultraviolet grade lenses, two $f=80$ mm planoconvex, and an $f=50$ mm biconvex, were used to focus the lamp beam to a rectangular image of a few mm^2. All devices except the lamp were mounted on a Newport Research, Inc. optical table.

The PDS probe beam was provided by an Optikon 2-mW He-Ne laser, LGK 7672, with an Optikon LM2P power supply. An $f=20$ mm planoconvex lens focused the probe beam as it passed over the WE. The probe laser was mounted on a tilting gimbal to allow careful alignment of the beam relative to the sample surface. The PDS beam deflection was detected by a United Detector Technology 431 X-Y position monitor, equipped with a UDT SC-25 quadcell; this detector was covered by a 632.8-nm (He-Ne wavelength) interference filter to minimize noise due to stray excitation light. The UDT 431 signal was fed into an Ithaco 1201 low-noise preamplifier for amplification and filtering. The ac signal from the preamp was then fed into an EG&G Princeton Applied Research model 5204 lock-in analyzer. The lock-in output in this, and other cases, was sampled by a computer driven analog-to-digital conversion board.

The ac photocurrent-bias apparatus consisted of a Solatron Schlumberger 1250 frequency response analyzer connected across a series combination of a reference resistor (about 10 Ω) and the PEC cell. The ac photocurrent across the reference resistor was monitored with a lock-in analyzer.

EXPERIMENTAL RESULTS AND DISCUSSION

In the theoretical section a PDS technique to determined the quantum efficiency of a PEC cell under dc bias was developed. In order to verify this result, PDS and PC data were obtained for several CdS electrode-polysulfide electrolyte systems; following the experimental measurements, Eqs. (13), (14), and (16) were applied to the data in order to determine Q_{max}, $(E_R - E_{VB}^S) + \Delta G$, and a semitheoretical $\Delta(V)/\Delta_{OC}$ versus $V - V_{FB}$ curve for each system.

It must be recalled that one of the assumptions used in our theory to justify the PDS method of determining Q_{max} was that the radiative quantum efficiency was zero; this assumption appears to be valid for CdS electrodes. For instance, Karas and Ellis[16] found that Ag- or Te-doped CdS gave a radiative Q of 10^{-4}–10^{-2}, and Streckert *et al.*[19] quoted a value of 10^{-4}, values close enough to zero for our purposes. Since the radiative quantum efficiency has been assumed to equal zero, the nonradiative quantum efficiency (Q_{nr}) is given by $1-Q$, where Q is the photocurrent quantum efficiency.

In some cases experimental $\Delta(V)$ data were normalized by the flatband PDS signal, Δ_{FB}, since, in theory, $\Delta_{FB}=\Delta_{OC}$ (the photocurrent quantum efficiency is zero in both cases). In addition, experimental PDS data have been smoothed using the following method: Each data point has been replaced by the average value of the data point and its two nearest neighbors. Moreover, although we have not presented any PDS phase versus bias data, the PDS phase was found to be independent of bias in all

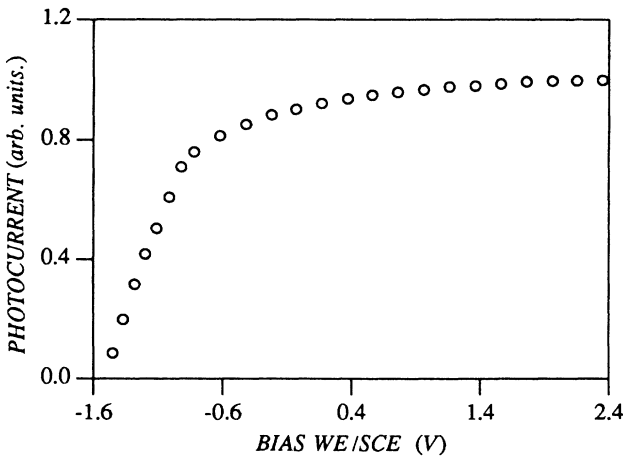

FIG. 2. ac photocurrent magnitude vs dc bias voltage for F-CdS in 0.05M PS; 490 nm; 25 Hz.

cases. Finally, several photocurrent versus bias curves have already been published[10] for the three CdS electrodes in question; a typical curve is shown in Fig. 2.

A. PDS bias measurements in 0.01*M* PS

Figures 3(a)–3(c) show experimental and semitheoretical $\Delta(V)/\Delta_{OC}$ versus $V-V_{FB}$ curves for all three samples in 0.01*M* PS, at 25 Hz. Since the semitheoretical curves were fitted to the experimental curves in the linear, high-bias region, it is not surprising that the correlation between the semitheoretical and experimental curves is best in that region.

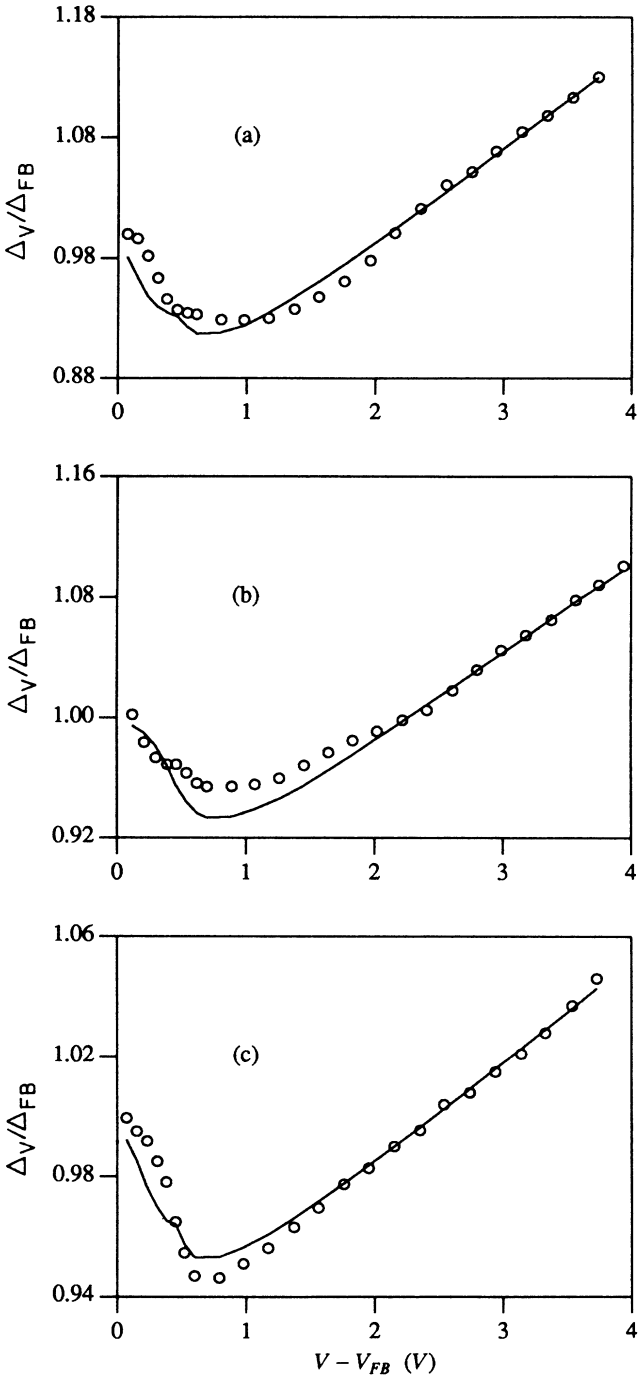

FIG. 3. Experimental (○) and semitheoretical (solid line) Δ_V/Δ_{FB} vs $V-V_{FB}$ (V) curves for CdS in 0.01*M* PS and $f=25$ Hz: (a) F-CdS, 490 nm; (b) Ga-CdS, 490 nm; (c) LR-CdS, 480 nm.

TABLE I. Q_{max} and $(E_R-E^S_{VB})+\Delta G$ values determined from PDS versus bias measurements in 0.01*M* PS.

Electrode	λ (nm)	V_{FB} (V/SCE)	Q_{max}	$(E_R-E^S_{VB})+\Delta G$ (eV)
F-CdS	490	−1.55	0.20	0.31
Ga-CdS	490	−1.60	0.15	0.14
	480	−1.60	0.24	−0.19
LR-CdS	480	−1.55	0.09	−0.06

Table I shows the values of Q_{max} and $(E_R-E^S_{VB})+\Delta G$ obtained from the experimental curves in 0.01*M* PS; note that the quoted V_{FB} values were calculated by extrapolating the photocurrent versus bias curves to the voltage axis. Before the table is examined, an approximate value for $(E_R-E^S_{VB})+\Delta G$ will be calculated independently from experimental potential measurements. First, $E_R=-0.8$ V saturated calomel electrode (SCE) (the potential of a CdS electrode in polysulfide solution); changing to a potential on the neutral hydrogen electrode (NHE) scale, $E_R=-0.56$ V/NHE, and converting to energy units, $E_R=-4.14$ eV/vacuum. Also, $E^S_{CB}\approx-1.55$ V/SCE (from Table I V_{FB} values); changing to a NHE potential, $E^S_{CB}=-1.31$ V/NHE, and in energy units, $E^S_{CB}=-3.39$ eV/vacuum. Also, $E^S_{CB}-E^S_{VB}=E_g$, where $E_g=2.4$ eV. Finally, $\Delta G=nV_R$, where n is the number of electrons participating in the redox reaction, V_R is the oxidation potential (V/NHE) of the redox reaction, and ΔG has units of eV; assuming $n=2$ ($2S^{2-}\rightarrow 2e^-+S_2^{2-}$), $\Delta G=2\,(-0.56)=-1.12$ eV. Therefore $(E_R-E^S_{VB})+\Delta G=0.53$ eV.

The first observation from Table I is that all of the values of Q_{max} were quite low (<0.25); this result can be attributed to the photocorrosion which dramatically affected the electrodes in 0.01*M* PS. For the Ga-CdS, as the wavelength was decreased from 490 to 480 nm, Q increased from 0.15 to 0.24, and $(E_R-E^S_{VB})+\Delta G$ did not change significantly, as expected. Overall, none of the $(E_R-E^S_{VB})+\Delta G$ values were very close to the expected 0.53 eV.

B. PDS bias measurements in 0.05*M* PS

Figures 4(a)–4(c) show experimental and semitheoretical $\Delta(V)/\Delta_{OC}$ versus $V-V_{FB}$ curves for the three CdS electrodes in 0.05*M* PS, at 25 Hz. As noted above, the correlation between the experimental and semitheoretical curves is best at high bias, where the two curves were fitted. Also, the curves showed anomalous downturns (of varying degree) as the bias was decreased near V_{FB}, an effect attributed to photogenerated electrochemical species gradients; a species gradient would tend to push the probe beam away from the electrode,[20] decreasing the thermal PDS signal.[3] Large dc forward-bias currents were observed[10] to be induced in 0.05*M* PS, but not in

0.01M PS, which explains why the forward-bias PDS anomaly was not observed in the 0.01M PS.

With regard to the Q_{max} and $(E_R - E^S_{VB}) + \Delta G$ data collected in Table II, for the F-CdS and Ga-CdS samples, Q_{max} increased as the wavelength was decreased; this trend is in keeping with the well-known Gartner model[21] for PEC-like systems. The Gartner model predicts that as the absorption coefficient increases (i.e., the wavelength decreases in the vicinity of the CdS band edge), the PC quantum efficiency increases, due to the fact that a greater number of photons are absorbed within the depletion layer, where 100% collection efficiency is assumed to exist. Furthermore, all of the $(E_R - E^S_{VB}) + \Delta G$ values were in the range 0.76 to 1.77 eV, significantly higher than the expected value of 0.53 eV; all three electrodes had $(E_R - E^S_{VB}) + \Delta G$ values which were considerably higher in 0.05M PS than in 0.01M PS. Also, all of the electrodes had higher Q_{max} values in 0.05M PS than in 0.01M PS, which attests to the better corrosion protection offered by the 0.05M PS. Finally, the Ga-CdS crystal had the highest quantum efficiency in both electrolytes.

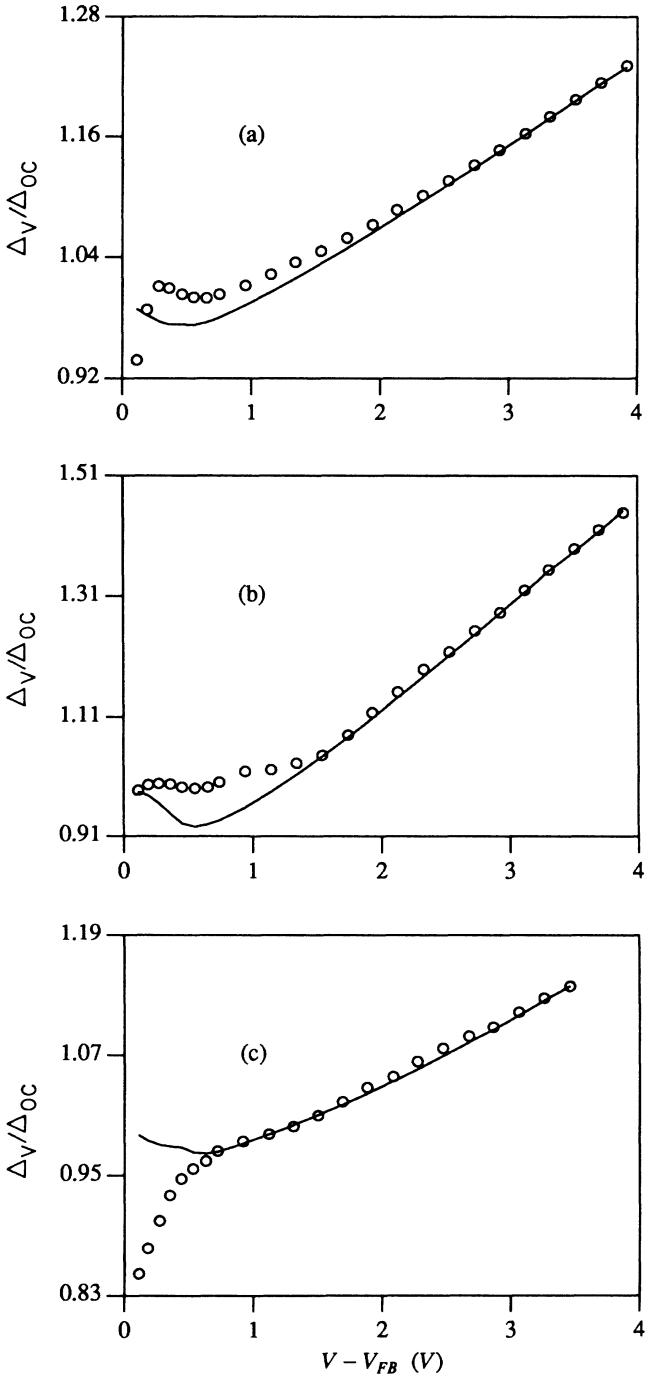

FIG. 4. Experimental (○) and semitheoretical (solid line) Δ_V/Δ_{OC} vs $V - V_{FB}$ (V) curves for CdS in 0.05M PS and $f = 25$ Hz: (a) F-CdS, 480 nm; (b) Ga-CdS, 480 nm; (c) LR-CdS, 490 nm.

TABLE II. Q_{max} and $(E_R - E^S_{VB}) + \Delta G$ values determined from PDS versus bias measurements in 0.05M PS.

Electrode	λ (nm)	V_{FB} (V/SCE)	Q_{max}	$(E_R - E^S_{VB}) + \Delta G$ (eV)
F-CdS	515	−1.50	0.10	0.76
	510	−1.50	0.16	0.83
	490	−1.50	0.21	1.09
	480	−1.56	0.21	1.33
	500	−1.50	0.19	1.49
Ga-CdS	490	−1.55	0.35	1.35
	480	−1.55	0.44	1.15
	470	−1.45	0.44	1.77
LR-CdS	490	−1.53	0.16	1.10

C. PDS load measurements

The WE PDS signal was also measured as a function of load resistance, but little variation in the PDS signal was observed as the load was varied. It appears that the PDS technique is not well suited for determining the energy efficiency (EE) of PEC cells: (a) There is no simple way of relating the PEC EE to the PDS signal, as could be done for the solid-state photovoltaic cell, (b) if Eq. (22) is to be used to determined the PEC EE, the ΔG heating term must be estimated, and (c) the presence of a photogenerated species gradient in the electrolyte will perturb the thermal PDS signal, making it difficult to observe the small variation in the PDS signal due to optical to electrical energy conversion. Fujishima *et al.*[4] have obtained a type of energy efficiency, measured under dc bias, which was quite different from the EE described here. Their method, which employed a thermistor to measure the dc temperature change in the vicinity of the WE due to a step-input optical excitation, was simpler than the PDS method presented here, because only a dc current or voltage component had to be dealt with. Unfortunately, they did not measure the EE under load, so their results cannot be directly compared with ours.

CONCLUSIONS

In this work experimentally derived values of Q_{max} and $(E_R - E^S_{VB}) + \Delta G$ were examined. The Q_{max} values were found to be quite low (< 0.45), compared to literature

values[4] (≈ 1.0), which is not surprising taking into account the anodic corrosion which was observed to take place on the WE surface. Fujishima *et al.*[22] have compared the quantum efficiencies obtained using a thermistor photothermal technique with those obtained using a photon-counting actinometric method; they found that the thermal method for finding Q gave values greater than or equal to those obtained via the photon-counting technique. Generally, the photon-counting method will yield smaller values for Q because it counts all photons incident upon the electrode, while the thermal methods do not count photons reflected away from the electrode.

The PDS-derived $(E_R - E_{VB}^S) + \Delta G$ values varied over a wide range, and did not take on the expected constant value of 0.53 eV. Obviously, our simple model of the PDS signal, as a function of applied bias, was not complete enough to truly predict the PDS signal over a wide range of conditions (i.e., varied wavelength, bias, ionic species gradients). The accuracy of the PDS-derived $(E_R - E_{VB}^S) + \Delta G$ values is open to question due to uncertainty regarding the correct value of ΔG (the actual redox reaction occurring at the WE was unknown). However, the present model is an improvement over that by Fujishima *et al.*[4] and Maeda *et al.*,[11] who only fitted a linear expression to their ΔT versus V data (where ΔT is the temperature change measured at the WE with a thermistor) in the high-bias (V) region, and not over the whole range of V.

Overall, the PDS-derived quantum efficiency values were probably quite reliable, although the PDS technique is not likely to replace the traditional photon-counting technique as the preferred method for quantum efficiency determinations. One advantage of the PDS method is that it measures the internal quantum efficiency, which is only a function of the electronic behavior of the system, not the extent to which the light is reflected away from the electrode. The satisfactory correlation of the experimental data with the semitheoretical curves supported the validity of the employed PEC cell heat-generation model, increasing our confidence in the measured quantum efficiency values. The observed experimental inconsistencies in the value of $(E_R - E_{VB}^S) + \Delta G$ were probably due to photoelectrochemical species gradients; the species gradients were found to be quite time dependent, adding noise to, and decreasing the repeatability of the PDS signal. In this respect, a temperature sensing probe which was only sensitive to temperature (i.e., a thermistor) would have probably provided more reliable values of Q_{max} and $(E_R - E_{VB}^S) + \Delta G$. On the other hand, a thermistor is intrusive; it must be placed very close to the WE, increasing the chance that it will absorb incident or reflected light, leading to spurious signals. The PDS technique does not suffer from this problem since it is only sensitive to temperature gradients. Finally, the PDS load measurements suffered from the same problems detailed above for the PDS bias tests, and did not yield much useful information about the PEC cell.

ACKNOWLEDGMENTS

The authors wish to acknowledge the partial support of the Ministry of Energy, Mines, and Resources (EMR Canada) through an equipment loan from the Center for Hydrogen and Electrochemical Studies (CHES). Partial financial support by the Natural Sciences and Engineering Research Council of Canada (NSERC), and the Ontario Laser and Lightwave Research Center (OLLRC) is gratefully acknowledged.

[1] *Photoacoustic and Thermal Wave Phenomena in Semiconductors*, edited by A. Mandelis (North-Holland, New York, 1987).
[2] A. Mandelis, J. Appl. Phys. **54**, 3404 (1983).
[3] R. E. Wagner and A. Mandelis, Appl. Spectrosc. (to be published).
[4] A. Fujishima, Y. Maeda, K. Honda, G. H. Brilmyer, and A. J. Bard, J. Electrochem. Soc. **127**, 840 (1980).
[5] A. B. Ellis, S. W. Kaiser, and M. S. Wrighton, J. Am. Chem. Soc. **98**, 6855 (1976).
[6] A. B. Ellis, S. W. Kaiser, J. M. Bolts, and M. S. Wrighton, J. Am. Chem. Soc. **99**, 2839 (1977).
[7] A. L. Fahrenbruch and R. H. Bube, *Fundamentals of Sola. Cells—Photovoltaic Solar Energy Conversion* (Academic, New York, 1983).
[8] J. L. Boone and G. Cantwell, J. Appl. Phys. **57**, 1171 (1985).
[9] A. Mandelis and E. K. M. Siu, Phys. Rev. B **34**, 7209 (1986).
[10] R. E. Wagner and A. Mandelis, J. Electrochem. Soc. (to be published).
[11] Y. Maeda, A. Fujishima, and K. Honda, Bull. Chem. Soc. Jpn. **55**, 3373 (1982).
[12] D. Cahen, Appl. Phys. Lett. **33**, 810 (1978).
[13] J. Powderly (private communication).
[14] R. H. Bube and S. M. Thomsen, J. Chem. Phys. **23**, 15 (1955).
[15] R. W. Smith, Phys. Rev. **97**, 1525 (1955).
[16] B. R. Karas and A. B. Ellis, J. Am. Chem. Soc. **102**, 968 (1980).
[17] G. Hodes, J. Photochem. **29**, 243 (1985).
[18] S. Licht and J. Manassen, J. Electrochem. Soc. **132**, 1076 (1985).
[19] H. H. Streckert, J. Tong, M. K. Carpenter, and A. B. Ellis, J. Electrochem. Soc. **129**, 772 (1982).
[20] A. Mandelis and B. S. H. Royce, Appl. Opt. **23**, 2892 (1984).
[21] W. W. Gartner, Phys. Rev. **116**, 84 (1959).
[22] A. Fujishima, Y. Maeda, and K. Honda, Bull. Chem. Soc. Jpn. **53**, 2735 (1980).